2019 NDIA GROUND VEHICLE SYSTEMS ENGINEERING AND TECHNOLOGY SYMPOSIUM
MATERIAL AND ADVANCED MANUFACTURING TECHNICAL SESSION
AUGUST 13-15, 2019 - NOVI, MICHIGAN

Feasibility of Joining Wrought Homogenized Armor Steel with Friction Stir Welding

William Evans 1, Antonio Ramirez 1, Martin McDonnell 2, Mike Eff 1

1 Department of Welding Engineering, The Ohio State University, Columbus, OH
2 U.S. Army Future's Command, Warren, MI
3EWI, Columbus, OH

Abstract

The United State Army employs several advanced armored combat vehicles, in a wide array of different environments, and applications. Armor steels are hard and are required to meet certain conditions to stay within the military's specifications for armored steels. Vehicle armor is typically joined using arc welding methods. Joining via arc welding degrades armor material below specification, so alternate joining methods are being explored like Friction Stir Welding (FSW). FSW is a solid-state joining technique that utilizes a rotating pin to stir plasticized material and use a tool shoulder to forge the material into the joint. The advantages come from the reduction in peak temperature, an increase in mechanical performance, and a decrease in possible defects that occur. In this study FSW parameters were developed and used to weld Wrought Homogenous Armor (HRA) steel. The welds were subject to hardness indention, and metallographic analysis to observe an early prediction of joint properties. Through this work it was shown that HRA can be joined using FSW and the weld stir zone is similar in properties to the base metal.

Citation: W. Evans, A. Ramirez, M. Mcdonnell, M. Eff, "Feasibility of Joining Wrought Homogenized Armor Steel with Friction Stir Welding", *In Proceedings of the Ground Vehicle Systems Engineering and Technology Symposium* (GVSETS), NDIA, Novi, MI, Aug. 13-15, 2019.

1. Introduction

In recent years there has been a considerable effort to reduce the weight of armored vehicles for both efficiency and for performance of said vehicles. This effort has brought on a need to research new emerging materials and processes for vehicle fabrication. One such fabrication process pertains to the joining of armor steels. In general, arc welding is used extensively for joining armor steel for vehicle fabrication. The high peak temperatures and act of solidification can introduce many defects as well as severely altering the performance of the armor grade steel in regions adjacent to the weld. In addition to these issues a non-matching filler metal is often used when

welding these steels. This will further change the properties of the welded joint. A possible replacement for arc welding is Friction Stir Welding (FSW).

FSW is a solid-state joining process that utilizes a non-consumable tool to frictionally heat and deform the welded material into a consolidated joint [1], [2]. Figure 1 displays a diagram showing the process forces and an overview of the FSW process. FSW by nature is an autogenous weld negating any problems with using dissimilar filler metals [1], [3], [4]. The ability to join these steels in the solid-state also bring many additional benefits. With this process all hot cracking defects will be eliminated as well as hydrogen induced cracking defects [1], [5]. The lower peak temperature observed in this process also has the potential to reduce the width of the weld HAZ but will not be able to eliminate it[6].

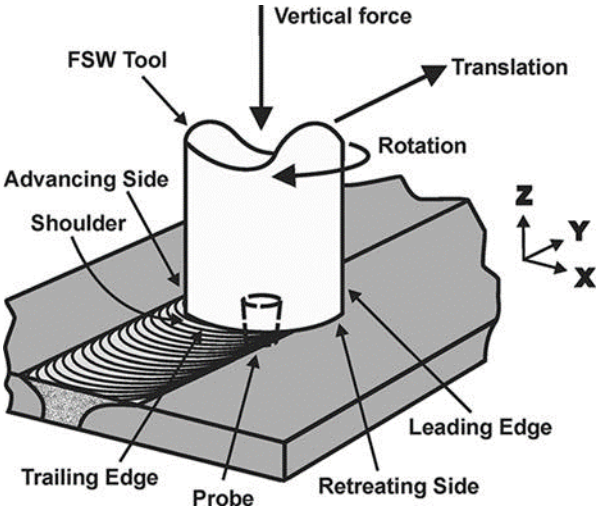

Figure 1 Diagram of the FSW process. Denoting the terminology for the different parts of the FSW tool and the coordinate system used in this work.

Since its invention a large amount of research has been conducted on the FSW process. Today this process is readily used to weld Al, Cu and some Mg alloys [3], [7]. Their low hardness and low plasticization temperature make these alloys ideal for this welding process. Another reason for using FSW on these alloys are they are often referred to as "un-weldable" through conventional joining procedures [3].

In addition to the alloys mentioned above many other metals have been successfully joined using FSW. Harder materials such as carbon steel, stainless steel, Ni-base alloys, and Ti-base alloys have all been joined in a laboratory setting successfully [1], [4], [8], [9].

A large interest in industry with regards to joining steels with FSW has been shown in the past. Examples of some of the interested sectors of industry are the pipeline production, maritime ship building, and automotive industry [10]– [14]. Past research has found favorable joint tensile strength, a reduction in weld joint distortion, and an elimination of fusion related defects [1], [12], [15], [16]. Good toughness values have been reported in low alloy carbon steel FSW joints as well [17]– [21]. That being said, a variety of joint properties can be found in carbon steel systems depending on the parameter set used to create said FSW joints [14], [22], [23]. Due to this fact is it necessary to optimize the parameters used to create these joints, which is often very costly.

Figure 2 displays a cross section of a FSW created in a carbon steel [17]. The weld center is referred to as the stir zone (SZ), this is the region where the FSW tool traveled. The material in the SZ is actively deformed and mixed together to form a consolidated joint. The thermo-mechanical affected zone (TMAZ) refers to the region in the HAZ that is deformed but not mixed into the joint. The TMAZ observed the highest temperature in the HAZ and observes some grain

reorientation. The HAZ can be broken down into a high temperature HAZ and a low temperature HAZ. Figure 2 denotes the high temperature HAZ, but outside of this region there is a lower temperature HAZ which is relevant when welding on martensitic steels.

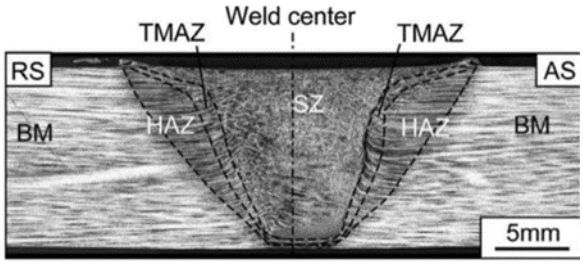

Figure 2 Cross section of a steel FSW with each of the regions of the weld labeled.

The main drawback to using FSW to join steels is the initial cost of equipment and the high cost of FSW tools. It is necessary for the FSW tools to exhibit high temperature mechanical and chemical properties when using them to join steel. Researchers have mainly focused on two tool materials Polycrystalline boron nitride (PCBN), and tungsten (W) based tools [1], [9], [24], [25]. PCBN based tools are known for their high wear resistance but limited to low ductility, PCBN being the second hardest material on earth behind diamond. Tungsten based tools have been shown to have good toughness but wear much faster than PCBN so they must be re dressed more often. Both tool materials are very expensive and difficult to manufacture. So, for this process to be feasible in steels the cost of the tool must beoffset by the cost savings of using the process.

Previous studies have been conducted on the overall economic advantage of using FSW [26]. One such study conducted by Fairchild et al. found that there were cost savings when using FSW to join steel pipelines. Up to 30% cost savings were found when switching from arc welding to FSW for offshore pipeline joining. The main idea behind cost savings are the thicker the plate being welded the higher the savings. This is due to the reduction in welding time and man hours involved when reducing multiple arc welding passes with a single FSW pass.

This study has been focused on joining rolled homogenized armor grade steels (RHA) specified under MIL-DTL-12560[27]. This material is readily used on several armored vehicles and due to its wide use, it was designated as a good material to conduct a proof of concept or a feasibility study with.

2. Experimental Procedure

For this experiment RHA was procured in the form of 12.5mm thick plates. The material's chemical composition was found using OES and is displayed in Table 1. The material was received and welded in the quenched and tempered martensitic state.

Table 1 Chemical composition of the RHA steel used for this experiment

C	Si	Mn	P	S	Cr	Mo	Ni	Al	Co
0.29	0.3	0.62	0.01	0.0008	0.93	0.35	0.42	0.039	0.006
Cu	Nb	Ti	V	Pb	Sn	As	N	Bi	Fe
0.14	0.003	0.003	0.004	0.002	0.007	0.006	0.008	0.002	96.8

All welding was conducted using an Accustir FSW machine attached to a gantry system at EWI. Welding was split into two different phases for this work. Initially welds were made in the bead on plate
configuration to develop parameters for adequate stirring and consolidation of the RHA material. The next phase of the research saw the joining of two plates using down selected parameters from the initial phase of the work.

For bead on plate welding the surface of the pates were ground and sand blasted to remove any scale and oxide. Before welds were conducted a pilot hole was drilled at the

weld plunge location. This was done to reduce the wear on the tool during the initial plunge section of the weld.

During the second phase for creating deliverable welds each plate surface was ground and sand blasted to remove oxide and scale also. In addition, each mating surface was machined flat for joint fit up. Pilot holes were also used to reduce weld plunge forces.

All welds were created using a PCBN based FSW tool containing 70% PCBN with 30% W-Re used as a binding agent. The tools used during this project had a pin with counterclockwise threads with three flats and a scrolled convex shoulder geometry. A drawing of the FSW tool is shown in Figure 3. To protect the FSW tool material 99.998% argon was delivered to the FSW tip using a gas diffuser. During parameter development a chamber was used to contain the shielding gas around the plate and tool. In the deliverable welding trials a shielding gas delivery system was used to deliver argon directly to the tool.

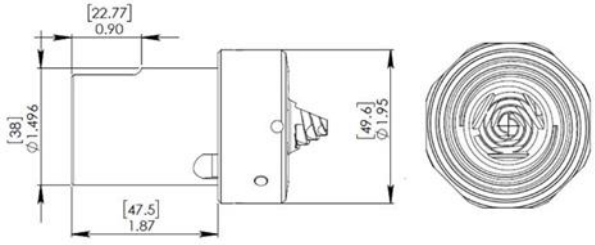

Figure 3 Drawing of the FSW tool utilized in the experiment. Compliments of MegaStir inc.

The methodology for developing parameters consisted of iterating between varying welding RPM and tool plunge depth. Visual inspection was conducted during the weld and after the weld, when a portion of the weld exhibited adequate characteristics regarding surface quality, level of flash, and lack of defects the plunge force was recorded. Plunge force was utilized to create consistent welds for previous iterations of development. The idea behind setting a constant plunge force is to maintain the same level of tool engagement throughout the entire weld section.

After down selecting, welding parameter destructive analysis and radiography were used to examine the interior of the FSWs. This was to confirm that no internal defects were present before moving forward to making deliverable welds in the next phase of the project.

Four welds were conducted in the second phase of the project. The final two welds were utilized for all joint performance evaluation in the form of mechanical and metallographic inspection.

Cross weld tensile testing, Charpy v-notch (CVN), and micro hardness indention were used to evaluate the mechanical performance of these welded joints. Optical microscopy and SEM were used to conduct metallographic analysis of the deliverable welds.

Tensile testing was conducted using samples from deliverable weld No. 3 and the reduced section specimen geometry displayed in Figure 4. This geometry was chosen to maximize the distance between the HAZ and the radius section of the dog bone shape. All testing was conducted using a Baldwin tensile testing frame with a capacity of 120 kip.

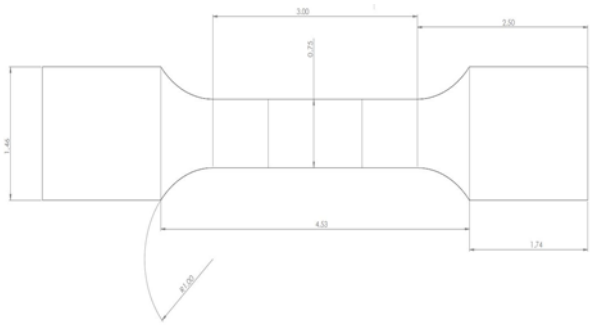

Figure 4 Drawing of cross weld tensile sample geometry.

CVN testing was conducted in accordance to ASTME E23 using full size specimens with dimensions 10 mm x 10mm x 55mm. Ten specimens were extracted from the center of deliverable welds No. 3 and No. 4 for a total of twenty samples. In addition, five samples were taken from as received base material in the same orientation as were taken from the welded joints. Between the ten samples from the welded joints five were notched in the center of the SZ and five were notched in the high temperature HAZ. All testing was conducted at -40C in accordance with MIL-DTL-12560.

Micro hardness indention was conducted on parameter development weld No. 5 and deliverable welds No. 3 and No. 4. Hardness indention was carried out with a Vickers diamond shaped indenter at 1kg load with an indent spacing of 500 microns. A map was created of each welded joint.

3. Results

3.1 Parameter Development

Table 2 displays the parameters used during the initial phase of development used to down select parameters for deliverable welding. Weld No. 1 and 2 utilized position control welding to find adequate tool position for a quality surface and no defects present. Upon visually inspecting weld No. 2 a section at the end of the weld met the quality criteria set in place. Examining the force trace of the weld, shown in Figure 4, the section at the end of the weld showed a plunge force of 29,000 lbs and a plunge depth of .51 inches. This was the setting used to conduct the rest of the welding trials where the focus was controlling heat input with RPM.

Table 2 Parameters used during development phase

	Plunge		Welding		
Weld Number	RPM	Dwell (s)	RPM	Travel Speed (in/min)	Control Type
1	450	0.5	200	4	Position
2	450	None	125	4	Position
3	450	None	100	4	Force
4	450	None	125	3.5	Force
5	450	None	75	2	Force

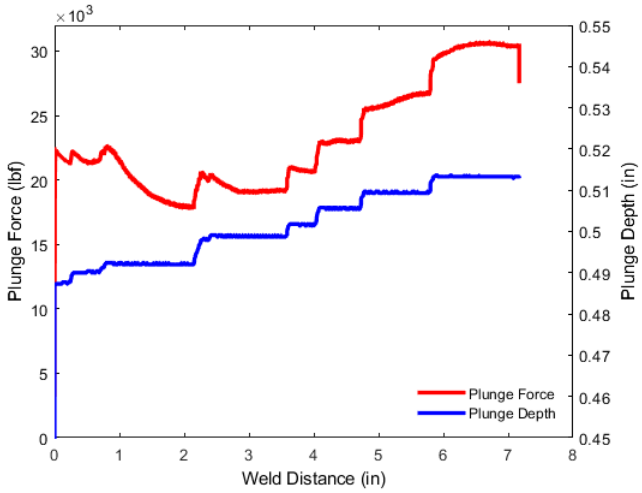

Figure 5 Process plunge force and plunge depth vs. weld distance for development weld No. 2.

Throughout all the welding trials RPM was reduced, this was to decrease the overall heat generated by the FSW process. The PCBN FSW tool ideally needs to stay below 1652°F (900°C) to maintain the mechanical integrity of the PCBN material. Examining Figure 5, the tool temperature recorded at the backside of the FSW tool shoulder, the weld operating temperature was significantly over this 1652°F (900°C) threshold. An example of the weld operating temperature is shown in Figure 6, which displays the thermal history of the FSW tool shoulder during weld No. 4.

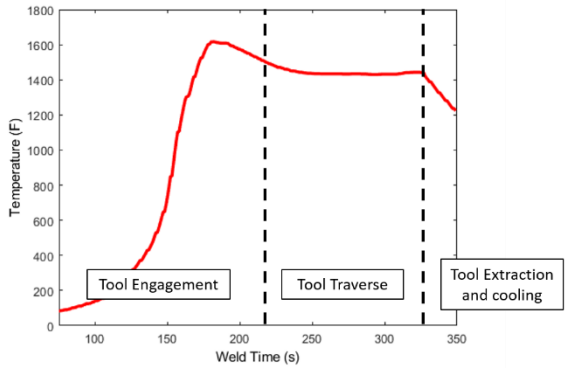

Figure 6 Example thermal history plot during development welding.

Parameter development welds No. 3 and 4 were cross sectioned to examine the specimens for any internal defects. A small worm hole defect was found at the end of weld No. 3, but not at the beginning section of the weld. The cross section of weld No. 3 is shown in Figure 7 and 8. A worm hole opened on the advancing side of the SZ.

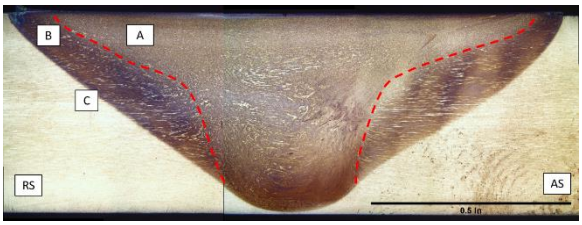

Figure 7 Cross section of development weld No. 3. This image depicts the first third of the weld where no defect was found.

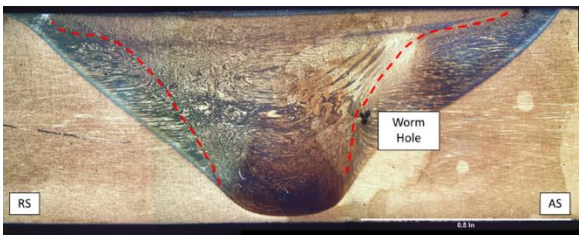

Figure 8 Cross section of development weld No. 3. This image depicts the last third of the weld where a worm hole defect was found.

A cross section of weld No. 4 can be observed in Figure 9. During this weld RPM was increased to attempt to increase material flow. The increase in material flow would remedy the defect observed in development weld No. 3. It can be observed that the defect disappeared in development weld No. 4. SEM images were also taken at the top of the SZ and bottom of the SZ to compare microstructure. A lathy martensitic microstructure was shown at the top and a fine grain martensitic microstructure was seen at the bottom of the SZ along the root of the weld.

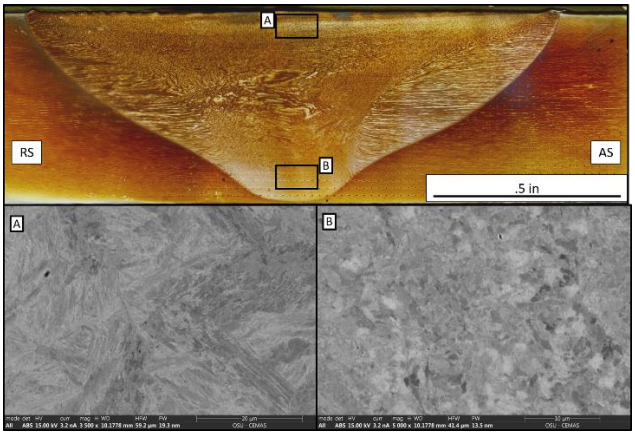

Figure 9 Cross section of development weld No. 4 with high magnification SEM images of the top and bottom of the SZ.

3.2 Deliverable Welding

From the parameter development section welding parameters were down selected for deliverable welding. The parameters used to create all the welded joints for testing were 125 RPM, 4 in/min, and 27,000 lbs of plunge force. With these parameters 4 welded joints were created. Of the four welded joints deliverable welds No. 3 and No. 4 were utilized for joint performance analysis. A cross section of Weld No. 3 is shown in Figure 10, the figure also displays the notch location for the CVN testing that was conducted. A force trace for deliverable weld No. 3 is displayed in Figure 11. The deliverable welds were 16 inches long with full penetration the entire length of the joint.

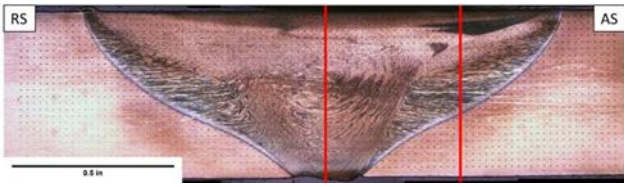

Figure 10 Cross section of deliverable FSW No. 3. Depicted on the image are the regions for each CVN notch location.

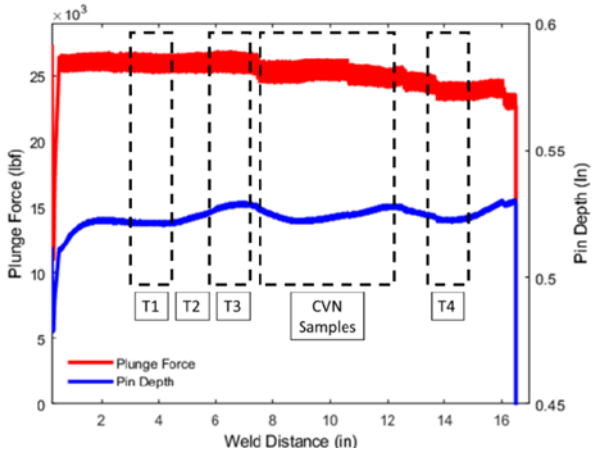

Figure 11 Weld Plunge force and Plunge depth for Deliverable weld No. 3. On the image is a diagram of where each specimen was taken for mechanical testing.

CVN impact results are displayed in Table 3. The table shows the impact energy in Joules for each plate and notch location, as well as an average between both plates, the average energy from the base metal and the minimum energy specified by MIL-DTL-12560.

Table 3 CVN testing results. All values shown are in J.

Plate A SZ	Plate A HAZ	Plate B SZ	Plate B HAZ
14.43	40.83	15.7	37.5
SZ Avg	**HAZ Avg**	**BM Avg**	**Min Energy**
15.07	39.17	49.78	16

Table 4 displays the results from cross weld tensile testing. The table displays weld UTS, elongation to failure, and the failure location for each tensile specimen. Figure 12 displays the resulting tensile bar specimens after pulling to failure.

Table 4 Cross Weld Tensile Test Results

Sample	UTS	Elongation to Failure	Failure Location
1	166033	1.40%	RS SZ
2	133247	0.50%	RS SZ
3	174754	5.00%	RS HAZ
4	117486	0.45%	RS SZ

Figure 12 Cross weld tensile specimens after failure.

Micro Hardness Mapping

Micro hardness mapping was conducted for three weld cross sections corresponding to parameter development weld No. 4 and deliverable weld No. 3 and No. 4. The resulting maps are displayed below in Figures 13-15. Each map was created toward the center section of each weld to capture the steady state region of the weld.

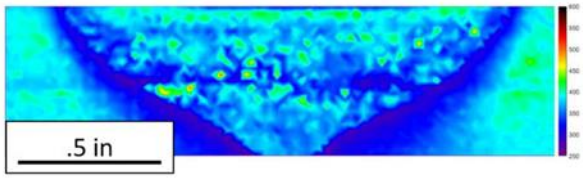

Figure 13 Micro hardness map of development FSW No. 4.

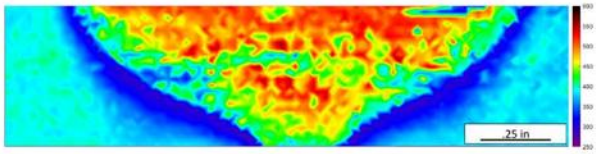

Figure 14 Micro hardness map of deliverable FSW No. 3.

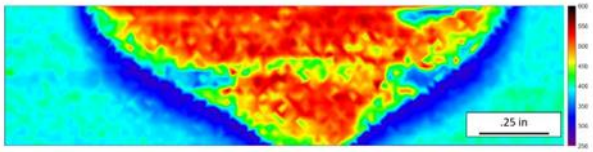

Figure 15 Micro hardness map of deliverable FSW No. 4

4. Discussion

During the parameter development phase of this experiment it was found that controlling the temperature of the weld was quite difficult using the set up that was available. This is what led to a reduction in welding RPM throughout the consecutive welds. When visually inspect the surface of parameter development weld No. 3 it appeared to have a nice surface, a low amount of material flash, and good shoulder engagement. This would indicate a good weld, but upon examining the exit hole a small worm hole defect was found. Further destructive analysis, through cross sectioning the weld, showed a worm hole formed in the last third of the weld. This was most likely caused by a drop off in weld temperature as the FSW tool traveled further away from the tool plunge location. The tool plunge location undergoes a large amount of heating and sees the peak temperature of the weld, upon full engagement the tool travels away from this region of high temperature. The parameters used in development weld No. 3 (100 rpm/4 in/min) must not have generated enough heat to keep the material flow high to eliminate welding defects. So, the next weld saw an increase in welding RPM to meet the need to increase material flow to remedy the defect. Upon radiographic and destructive analysis of development weld No. 4 the defect was eliminated, and those parameters were selected for deliverable welding.

The hardness results were quite different when comparing the parameter development welds and the deliverable welding. The as received quenched and tempered RHA exhibited hardness values around 400 HV. In the as quenched state RHA average hardness values of 561 HV. When

comparing the SZ and high temperature HAZ of the parameter development weld to the received base material the SZ was softened slightly in some areas but exhibited similar hardness values of 400 HV in others. This would indicate that the SZ and HAZ should exhibit similar properties to that of the base metal. In the low temperature HAZ of development weld No. 3 it can be observed that a decrease in hardness up to 100 HV can be observed. This is due to over-tempering of the already tempered martensite present in the base metal. When comparing the SZ and high temp. HAZ of the parameter development welds to the deliverable welds a drastic increase in hardness is observed. The SZ of the deliverable welds shows peak hardness values like that of the as quenched base material, or as quenched martensite. The SZ is much harder than that of the base metal. There is still a band of softened base metal in the low temperature HAZ like the development welds.

The drastic change in hardness can be attributed to several potential differences in welding conditions. The most likely cause is the fact that the deliverable welds were single passes on room temperature plates, while the developmental welds were done in the bead on plate configuration with multiple welds per plate. Due to this, there could be a

potential for the plate to be at a slightly elevated temperature when welding was conducted during parameter development. This could have allowed for some auto-tempering to occur in the SZ through a slower cooling rate. Other potential differences that could lead to an increase SZ hardness includes a slight change in travel speed, a difference in welding fixturing, a difference in ambient temperatures in the lab, etc. Regardless, the deliverable welds would indicate that a faster cooling rate was observed and the SZ exhibits hardness values like that of as quenched base material or as quenched martensite. This leads to a prediction of low toughness in the SZ due to the brittle nature of quenched martensite.

Examining the results of the CVN testing conducted the SZ averages are quite low around 14-15 joules. Both FSW SZ are below the minimum break energy required by MIL-DTL-12560, however only by one or two joules. Comparing to the base metal averages there is a much larger difference. The base metal exhibited an average break energy of over 49 joules. The low toughness is consistent with the hardness values recorded in the weld SZs, the microstructure in the SZ is made up of un-tempered martensite which is known to exhibit low toughness due to its brittle nature. Looking at the weld HAZ averages the toughness values increase closer to that of the base metal almost 10 joules difference between the two locations. These values are slightly misleading because the notch in the HAZ is a conglomerate of the SZ, high temp. HAZ, low temp HAZ, and base metal. This is due to the geometry of a conventional FSW. Taking from the hardness data, it is likely that the low temperature HAZ will exhibit higher toughness values compared to the SZ, and the high temperature HAZ will have slightly higher toughness than the SZ. However, the presence of some brittle SZ would reduce the overall break energy observed.

The results of the tensile testing show a variable specimen failure mode between a break directly through the SZ (specimen 1,2 and 4) and a more ductile failure with material yielding from the HAZ of the weld

(specimen 3). The cross weld UTS between the four samples ranged from 117 ksi to 174 ksi, with elongation from less than .5% to 5%. Overall the UTS values show promising values depending on the mode of failure. When loading of the specimens began a small gap appeared at the root of the sample of specimens 1,2, and 4 before final failure occurred. It is believed that this gap was either a defect present at the root of the weld or a soft region in the HAZ adjacent to the SZ acting as a stress concentration and leading to premature failure. The crack initiating at the root had an easy path to follow directly through the brittle SZ of these welds.

Examining the graph with the force trace of deliverable weld No. 3, the regions where each specimen were extracted is shown. Tensile specimen 3 exhibited the highest penetration depth and did not fail through the SZ of the sample. In addition to this an insignificant amount of material was removed from the root and face of the sample when machining the final specimen geometry. This would indicate that a defect was present at the root of these welds caused by either lack of penetration or backing plate material being present at the root face of the weld causing a stress concentration.

When comparing the tensile data to a bank of data gathered by the U.S. Army on the cross weld UTS of different GMAW filler wires the average UTS of the FSW matches that of the highest strength filler wire, that of

ER140S. A chart shown in Figure 13 shows a comparison to a few FM tested in this study are shown adjacent to that of the FSW UTS. The ER 140S filler metal was also the only filler material where the failure occurred in the HAZ. The promising result shown from these tensile testing is that specimen 3 exhibited an ideal failure mode while also having the highest elongation and UTS values.

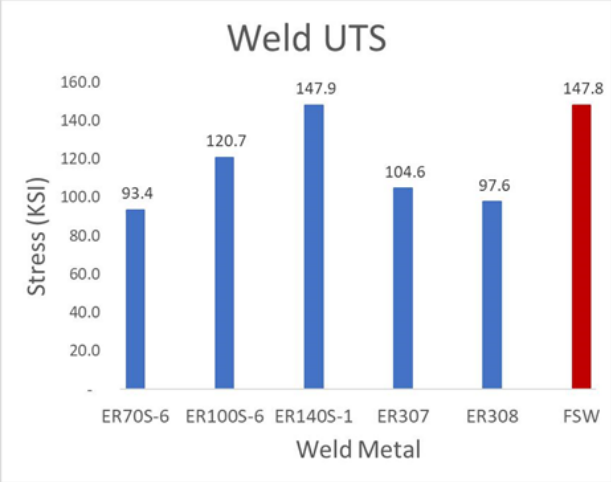

Figure 16 Cross weld UTS comparison to a study conducted by the U.S. Army on different steel filler material.

The issue with tensile testing RHA steels is that the UTS and yield strength is not called out in MIL-DTL-12560. This leads to a wide range of UTS values for steels that can be considered RHA. A few studies in literature show a range of RHA UTS values from 230 ksi – 319 ksi with elongations from 4-14% [28]– [31]. In addition to this range in properties the material composition ranges are just as wide.

5. Conclusions

Examining all the mechanical data gathered from this study it can be shown that FSW has a potential to be a good option for joining RHA. The main issue is the low toughness values in the SZ. The brittle SZ is most likely due to the welding procedure which could be altered for better performance. In addition, a tempering cycle could be introduced to decrease hardness values in the SZ to increase the toughness. Some additional conclusions that can be drawn from this study are:

- RHA can feasibly be joined using conventional FSW methods.
- When conducting single pass FSWs on RHA the SZ can become extremely hard and brittle. An additional thermal cycle, in the form of pre/post weld heat treatment, is needed to reduce SZ hardness.
- The SZ CVN results are below minimum requirements in MIL-DTL-12560 but only by 1-2 joules. The HAZ CVN values meet the requirements for toughness.
- Cross weld UTS values are acceptable when comparing to conventional filler materials used to join RHA in industry.

References

[1] F. C. Liu, Y. Hovanski, M. P. Miles, C. D. Sorensen, and T. W. Nelson, "A review of friction stir welding of steels: Tool, material flow, microstructure, and properties," *J. Mater. Sci. Technol.*, vol. 34, no. 1, pp. 39–57, 2018.

[2] L. Cui, C. Zhang, Y. chang Liu, X. guo Liu, D. po Wang, and H. jun Li, "Recent progress in friction stir welding tools used for steels," *J. Iron Steel Res. Int.*, vol. 25, no. 5, pp. 477–486, 2018.

[3] Z. Y. Ma, A. H. Feng, D. L. Chen, and J. Shen, "Recent Advances in Friction Stir Welding/Processing of Aluminum Alloys: Microstructural Evolution and Mechanical Properties," *Crit. Rev. Solid State Mater. Sci.*, vol. 43, no. 4, pp. 269–333, 2018.

[4] G. K. Padhy, C. S. Wu, and S. Gao, "Friction stir based welding and processing technologies - processes, parameters, microstructures and applications: A review," *J. Mater. Sci. Technol.*, vol. 34, no. 1, pp. 1–38, 2018.

[5] J. J. Hoyos, V. F. Pereira, R. R. Giorjao, T. R. McNelley, and A. J. Ramirez, "Effect of friction stir welding on hydrogen content of ISO 3183 X80M steel," *J. Manuf. Process.*, vol. 22, no. April, pp. 82–89, 2016.

[6] X. Fei and Z. Wu, "Research of temperature and microstructure in friction stir welding of Q235 steel with laser-assisted heating," *Results Phys.*, vol. 11, no. October, pp. 1048–1051, 2018.

[7] M. Schwartz, "Friction stir welding," *Innov. Mater. Manuf. Fabr. Environ. Saf.*, no. February 2002, pp. 87–122, 2010.

[8] A. J. Ramirez and M. C. Juhas, "Microstructural Evolution in Ti-6Al-4V Friction Stir Welds," *Mater. Sci. Forum*, vol. 426–432, pp. 2999–3004, 2003.

[9] K. M. Venkatesh, M. Arivarsu, M. Manikandan, and N. Arivazhagan, "Review on friction stir welding of steels," *Mater. Today Proc.*, vol. 5, no. 5, pp. 13227–13235, 2018.

[10] A. O. A. Kumar, D. P. Fairchild, M. L. Macia, T.D. Anderson, H. W. Jin, R. Ayer, "Research Progress on FSW of Pipeline Steels.pdf." .

[11] A. M. El-Batahgy, T. Miura, R. Ueji, and H. Fujii, "Investigation into feasibility of FSW process for welding 1600MPa quenched and tempered steel," *Mater. Sci. Eng. A*, vol. 651, pp. 904–913, 2016.

[12] A. P. Reynolds, W. Tang, M. Posada, and J. Deloach, "Friction stir welding of DH36 steel," *Sci. Technol. Weld. Join.*, vol. 8, no. 6, pp. 455–460, 2003.

[13] J. Azevedo, L. Quintino, V. Infante, R. M. Miranda, and J. dos Santos, "Friction stir welding of shipbuilding steel with primer," *Soldag. e Insp.*, vol. 21, no. 1, pp. 16–29, 2016.

[14] T. W. Nelson, R. Steel, M. Gallagher, E. Olsen, and M. P. Miles, "Effect of friction stir welding conditions on properties and microstructures of high strength automotive steel," *Sci. Technol. Weld. Join.*, vol. 14, no. 3, pp. 228–232, 2009.

[15] S. P. J Perrett, J Martin, J Peterson, R Steel, "FSW of industrial Steels.pdf." .

[16] R. Steel, D. Fleck, T. Davis, S. Larsen, B. Johnson, and M. Mahoney, "Friction Stir Welding of 4340 Steel and 4340 Steel to Inconel 718," no. June, pp. 1–15, 2018.

[17] J. A. Avila, E. Lucon, J. Sowards, P. R. Mei, and A. J. Ramirez, "Assessment of Ductile-to-Brittle Transition Behavior of Localized Microstructural Regions in a Friction-Stir Welded X80 Pipeline

Steel with Miniaturized Charpy V-Notch Testing," *Metall. Mater. Trans. A Phys. Metall. Mater. Sci.*, vol. 47, no. 6, pp. 2855–2865, 2016.

[18] J. A. Avila, J. Rodriguez, P. R. Mei, and A. J. Ramirez, "Microstructure and fracture toughness of multipass friction stir welded joints of API-5L-X80 steel plates," *Mater. Sci. Eng. A*, vol. 673, pp. 257–265, 2016.

[19] T. F. A. Santos, T. F. C. Hermenegildo, C. R. M. Afonso, R. R. Marinho, M. T. P. Paes, and A. J. Ramirez, "Fracture toughness of ISO 3183 X80M (API 5L X80) steel friction stir welds," *Eng. Fract. Mech.*, vol. 77, no. 15, pp. 2937–2945, 2010.

[20] C. Sterling, T. Nelson, C. Sorensen, R. Steel, and S. Packer, "Friction Stir Welding of Quenched and Tempered C-Mn Steel," *Frict. Stir Weld. Proc. II*, no. June, pp. 165–171, 2003.

[21] A. Tribe and T. W. Nelson, "Study on the fracture toughness of friction stir welded API X80," *Eng. Fract. Mech.*, vol. 150, pp. 58–69, 2015.

[22] L. Wei and T. W. Nelson, "Influence of heat input on post weld microstructure and mechanical properties of friction stir welded HSLA-65 steel," *Mater. Sci. Eng. A*, vol. 556, pp. 51–59, 2012.

[23] T. W. Nelson and S. A. Rose, "Controlling hard zone formation in friction stir processed HSLA steel," *J. Mater. Process. Technol.*, vol. 231, pp. 66–74, 2016.

[24] M. Eff, "The Effects of Tool Texture on Tool Wear in Friction Stir Welding of X-70 Steel," 2012.

[25] H. K. D. H. Bhadeshia and T. DebRoy, "Critical assessment: friction stir welding of steels," *Sci. Technol. Weld. Join.*, vol. 14, no. 3, pp. 193–196, 2009.

[26] A. Kumar, D. P. Fairchild, M. L. Macia, T.D. Anderson, H. W. Jin, R. Ayer, A. Ozekcin, N. Ma, R. R. Mueller, "Evaluation of Economic Incentives and Weld Properties for Welding Steel Pipelines using FSW.pdf." .

[27] "Mil-Dtl-12560K," p. 12560.

[28] W. R. Whittington *et al.*, "Capturing the effect of temperature, strain rate, and stress state on the plasticity and fracture of rolled homogeneous armor (RHA) steel," *Mater. Sci. Eng. A*, vol. 594, pp. 82–88, 2013.

[29] S. J. Cimpoeru, "The Mechanical Metallurgy of Armour Steels," 2017.

[30] M. T. L. Tr, M. G. H. Wells, R. K. Weiss, J. S. Montgomery, and T. G. Melvin, "Materials Producibility Branch," 1992.

[31] I. Hardness, R. H. A. Weldability, and M. P. Testing, "Material Property Testing," *Office*, 1994.